DL-SIC: Deep Learning Aided Successive Interference Cancellation in Shared Spectrum

Zhiwu Guo, Wenhan Zhang, Ming Li, Marwan Krunz, and Mohammad Hossein Manshaei
Department of Electrical and Computer Engineering, University of Arizona, Tucson, Arizona, 85721, USA
Email: {zhiwuguo, wenhanzhang, lim, krunz, manshaei}@arizona.edu

***Abstract*—With the increasing demand for wireless capacity, multiple wireless technologies will inevitably coexist over shared bands. Successive interference cancellation (SIC) is a promising technique for improving spectrum utilization by utilizing the difference in the powers of concurrently received signals. However, enabling SIC over a shared band faces several challenges, related to the heterogeneity of the coexisting technologies, the unknown powers of received signals, and the uncoordinated and asynchronous nature of transmissions. Traditional SIC (T-SIC) receivers cannot simultaneously achieve low decoding latency and low decoding bit error rate (BER). To address these challenges, we propose DL-SIC, a deep learning approach for accelerating the operation of an SIC receiver. DL-SIC includes a deep learning-based protocol detector for identifying overlapping packets, as well as a deep learning-based SIC classifier for accurate determination of the SIC decoding order in scenarios where the relative strengths of the received signals are unknown. We conduct simulations and over-the-air (OTA) experiments to evaluate DL-SIC, and compare it with two T-SIC approaches, T-SIC$_1$ and T-SIC$_2$. Our simulation results clearly indicate that DL-SIC can simultaneously achieve low decoding latency and low decoding BER. Specifically, DL-SIC reduces decoding latency by 75.41% in the worst-case scenario and 84.44% in the best-case scenario compared to T-SIC$_1$. Furthermore, with a probability of approximately 60%, DL-SIC reduces decoding BER from 10^{-1} to 10^{-4} compared to T-SIC$_2$. Our OTA experiments further confirm the feasibility of DL-SIC.**

***Index Terms*—Spectrum sharing, successive interference cancellation, deep learning, SIC decoding order.**

I. Introduction

To cope with the growing demand for mobile data and the limited availability of licensed spectrum, both LTE and 5G systems have expanded their operations into the unlicensed 5 GHz and 6 GHz bands. A key requirement for such unlicensed operation is ensuring fair and harmonious coexistence with other incumbents, particularly Wi-Fi systems. For LTE, 3GPP standardized the License Assisted Access (LAA) [1], which employs a Listen-Before-Talk (LBT) mechanism at the MAC layer to coordinate access to the unlicensed channels. In Release 16, 3GPP introduced 5G New Radio Unlicensed (NR-U) [2] for unlicensed operation in the 5 GHz and 6 GHz bands.

This research was supported in part by NSF (grants # 2229386 and 1822071) and by the Broadband Wireless Access & Applications Center (BWAC). Any opinions, findings, conclusions, or recommendations expressed in this paper are those of the author(s) and do not necessarily reflect the views of NSF.

With these heterogeneous technologies (i.e., Wi-Fi, LTE-LAA, 5G NR-U[1]) sharing the same band, collision avoidance-based MAC protocols, such as LBT and carrier sense multiple access with collision avoidance (CSMA/CA), are often adopted. However, these protocols are known to suffer from low channel utilization [3]. To improve spectrum utilization, concurrent transmissions from heterogeneous systems may be allowed [4]–[7], which requires interference resolution strategies to mitigate cross-technology interference. Existing approaches for dealing with interference from heterogeneous technologies are mainly based on multiple-input multiple-output (MIMO) [4] and successive interference cancellation (SIC) [6], [7]. In contrast to a MIMO approach, SIC [7] does not require a multi-antenna capability; instead, it exploits the difference in the powers of concurrently received packets to decode these packets. The fundamental idea behind SIC is sequentially decoding received signals while iteratively canceling previously decoded ones.

A. Challenges and Motivation

Traditional SIC (T-SIC) receivers were originally developed for homogeneous (same-technology) coexistence [8], but later extended to heterogeneous coexistence of Wi-Fi/ZigBee [6] and LTE/Wi-Fi [7]. To motivate our work, we first describe how a T-SIC receiver may be extended to handle heterogeneous coexistence of Wi-Fi, LTE, and 5G NR protocols, using the example in Fig. 1. Depending on the assumed hardware capability, we consider two possible ways to implement a T-SIC receiver (other variations may also be envisioned):

(1) T-SIC$_1$: In this approach, cross-technology interference cancellation is performed after a frame is *fully received and correctly decoded*. As a result, in the worst-case, all possible SIC decoding orders may end up being considered. To illustrate, consider the situation in Fig. 1. After receiving a signal at time t_1, the T-SIC$_1$ receiver initiates three parallel detection processes, one per protocol, using auto-correlation and/or cross-correlation techniques. In this example, the LTE detector will be triggered first, and an LTE decoding process will commence right after t_1. Even though the three frame detectors may remain active while the LTE frame is being decoded, no action will be taken until the completion of this frame (at time $t_5 = t_1 +$ 10 msec). If LTE decoding

[1]For simplicity, in this paper, we use LAA, LTE, and LTE-LAA, interchangeably. The same is true for NR-U, 5G, and NR.

is successful (based on the outcome of the CRC) at t_5, the T-SIC$_1$ receiver will reconstruct the LTE signal and subtract it from the received composite signals. T-SIC$_1$ will then attempt to decode the next frame, as identified by one of the three detectors. In this example, it will be a Wi-Fi signal that starts at t_2. The same process is repeated. Note that additional samples that are received after t_5 need to be stored to facilitate the decoding of frames that last beyond t_5 (as is the case for the 5G NR frame in this figure). If the decoding of any given frame fails, the T-SIC$_1$ will consider a different SIC decoding order. For instance, if LTE frame decoding fails (as indicated by CRC failure) at t_5, the T-SIC$_1$ receiver will attempt to decode the Wi-Fi signal first, starting at t_2. After fully decoding the Wi-Fi frame at t_4, if this decoding is successful, T-SIC$_1$ will subtract the Wi-Fi signal from the composite signals and will attempt to decode an LTE frame using the remaining samples, starting at t_1. The overall decoding latency for T-SIC$_1$ can be significant due to its exhaustive nature (more on this in subsequent sections).

(2) T-SIC$_2$: In this approach, frame decoding is initiated *once the signal of any protocol has been detected*. As a result, multiple decoding processes may overlap in time, regardless of the relative strengths of the constituent signals. During the decoding of a given frame, decoded "chunks" from previously initiated decoding processes will be subtracted from the composite before the decoding of the current frame takes place, even if such chunks eventually fail the decoding process in their own respective decoders (at the time the frames are completely received). To illustrate, consider the situation in Fig. 1. Three frame detection processes will be simultaneously executed, one per protocol type. At t_1, an LTE signal will be detected, triggering an LTE decoding process. At t_2, a Wi-Fi signal may be detected by the second detector (in general, the detection threshold is much lower than the decoding threshold, so a weak non-decodable Wi-Fi signal may still be detectable). In contrast to T-SIC$_1$, Wi-Fi frame decoding will commence at this point, after subtracting a decoded chunk of the LTE signal that starts at t_2. A chunk here corresponds to a small portion of a frame, such as a subframe (1 msec). Thus, the decoding of the Wi-Fi frame commences at time $t = t_2+$ the chunk duration. The process continues until the detection of the 5G signal at t_3. At that point, 5G frame decoding can commence after subtracting chunks of partially decoded LTE and Wi-Fi signals. Note that the reconstructed and removed chunks may end up being inaccurate, but are still likely to reduce the interference and improve the BER of the decoded frame. Although this method has low decoding latency, it may result in a high decoding error rate for the LTE frame if the received signal strengths (RSS) of Wi-Fi and 5G NR are higher than that of LTE.

Designing a SIC receiver with both low decoding latency and low decoding error rate is challenging for several reasons:

(1) It is difficult to identify the protocol types for concurrently transmitted packets in real-time, given that heterogeneous protocols' transmissions in shared unlicensed bands are random. T-SIC assumes that the protocol types for concurrently transmitted packets are known in advance [6], which is impractical.

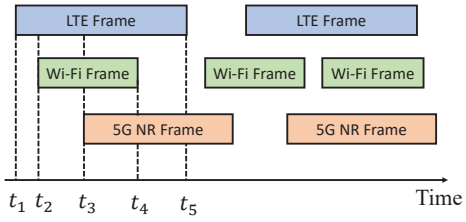

Fig. 1: Example of concurrent and asynchronous transmissions of Wi-Fi, LTE-LAA, and 5G NR-U. Frames have different received powers.

(2) Transmissions from different protocols are uncoordinated and asynchronous. Additionally, the RSS values of heterogeneous protocols' packets are unknown and may change due to channel fading and mobility, significantly impacting the real-time decoding order. T-SIC assumes a certain power order of the received signals [9], [10], which is impractical.

(3) T-SIC$_1$ incurs a large decoding delay to obtain the correct SIC decoding order information, whereas T-SIC$_2$ can decode packets in real-time, it may induce a high decoding error rate. This inherent trade-off between decoding latency and decoding error rate in T-SIC stems from not being able to identify the correct decoding order in real-time.

Therefore, a novel SIC architecture is needed to determine the SIC decoding order rapidly and efficiently.

B. Contributions

Our main contributions are summarized as follows:

(1) We introduce a novel DL-SIC receiver, which is comprised of a protocol detector and a SIC decoding order classifier. DL-SIC utilizes deep learning techniques to identify the protocol types and correct decoding order in real-time. We evaluate the performance of the proposed DL-SIC via extensive simulations.

(2) We analyze the decoding latency of both DL-SIC and T-SIC$_1$ in a three-protocol coexistence scenario (Wi-Fi, LTE, and 5G NR). Simulation results show that DL-SIC reduces the decoding latency by 75.41% to 84.44%, depending on the packet detection order and RSS order. Additionally, with a probability of approximately 60%, DL-SIC reduces decoding bit error rate from 10^{-1} to 10^{-4} compared to T-SIC$_2$.

(3) We validate the performance of DL-SIC using OTA experiments with USRPs (software-defined radio devices) for LTE/Wi-Fi spectrum sharing, demonstrating the practical feasibility of DL-SIC.

II. DL-SIC Architecture

A. System Model

Without loss of generality, we consider a heterogeneous coexistence scenario consisting of Wi-Fi, LTE-LAA, and 5G NR-U operating over the same 5 GHz unlicensed bands. Concurrent transmissions may occur due to hidden terminal

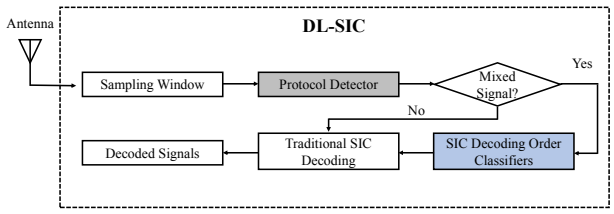

Fig. 2: Block diagram of DL-SIC, shaded boxes are new functions introduced by DL-SIC.

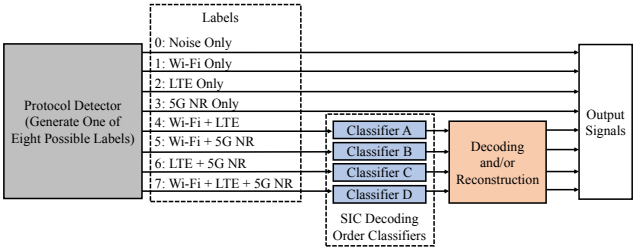

Fig. 3: Deep learning-based protocol detector.

problems or specific transmission strategies [4], [7]. Furthermore, receivers are capable of SIC decoding [7]. We focus on downlink transmissions and assume *unsaturated* traffic. The received signal at a given receiver is represented by:

$$y(t) = h_{\text{WiFi}}(t) \circledast x_{\text{WiFi}}(t) + h_{\text{LTE}}(t) \circledast x_{\text{LTE}}(t) + h_{\text{NR}}(t) \circledast x_{\text{NR}}(t) + n(t), \quad (1)$$

where $x_{\text{WiFi}}(t)$, $x_{\text{LTE}}(t)$, and $x_{\text{NR}}(t)$ are the transmitted signals of Wi-Fi, LTE, and 5G NR, respectively, at time t. The corresponding channels are denoted by $h_{\text{WiFi}}(t)$, $h_{\text{LTE}}(t)$, and $h_{\text{NR}}(t)$. $n(t)$ represents the thermal noise and other unaccounted interference. It is important to note that since the transmissions of all links are unsaturated, $x_{\text{WiFi}}(t)$, $x_{\text{LTE}}(t)$, and $x_{\text{NR}}(t)$ may be inactive at certain time t.

B. DL-SIC Design

1) Design Overview: The block diagram of DL-SIC is shown in Fig. 2, which includes a protocol detector and a SIC decoding order classifier, built on top of a traditional SIC receiver. Both components are based on deep learning. Upon sampling the received signal, the DL-SIC receiver feeds a window of baseband I/Q samples into the protocol detector, which identifies the protocol type(s) of the constituent signals. In the case of concurrent transmissions, multiple protocols will be identified. The output of the protocol detector is then used to select one of several classifiers, where each classifier predicts the decoding order of the mixed signals. Finally, the DL-SIC receiver decodes the mixed signals based on the predicted decoding order. If only one protocol is detected, DL-SIC decodes the signal following traditional SIC decoding procedures without utilizing the SIC decoding order classifier.

TABLE I: Layers Configuration of Adopted Neural Networks.

CNN Architecture	GRU Architecture
Conv2D, 128 neurons, with Average Pooling	GRU, 128 neurons
Conv2D, 128 neurons, with Average Pooling	GRU, 128 neurons
Flatten	Flatten
Fully-connected, 128 neurons	Fully-connected, 128 neurons
Fully-connected, 128 neurons	Fully-connected, 128 neurons
Output, Number of Classes	Output, Number of Classes

Both the protocol detector and SIC decoding order classifier can utilize three classic neural network (NN) architectures: Multi-Layer Perceptron (MLP), Convolutional Neural Network (CNN), and Gated Recurrent Unit (GRU) [11]. Note that Long Short-Term Memory (LSTM) [11] and GRU are two commonly used architectures in Recurrent Neural Networks (RNNs). Without loss of generality, we adopt GRU in this paper. The selection of these specific NN architectures for DL-SIC is underpinned by their representation and their widespread applicability across domains like image and RF signal classification, as well as sequential data analysis and prediction. The layers configuration of adopted NNs are shown in Table I. To facilitate a meaningful comparison between MLP and CNN (or GRU) architectures, we replace the two convolutional (or GRU) layers with two fully connected layers and adopt 128 neurons in each layer of the MLP architecture.

The DL-SIC receiver is capable of effectively detecting mixed waveform patterns that change dynamically in the time domain. Moreover, it can determine the SIC decoding order of constituent signals in an adaptive manner without requiring any prior knowledge of their RSS.

2) Protocol Detector: The I/Q samples in each sampling window vary over time due to the asynchronous transmissions of various protocols. In our three-protocol scenario, there are eight possible classes (combinations): Noise only, Wi-Fi only, LTE only, 5G NR only, Wi-Fi + LTE, Wi-Fi + 5G NR, LTE + 5G NR, and Wi-Fi + LTE + 5G NR.

Fig. 3 provides an overview of the protocol detector and its relationship with other components in DL-SIC. SIC is unnecessary if the protocol detector predicts only one technology, such as Labels 1, 2, and 3 depicted in Fig. 3. However, if the protocol detector predicts concurrent transmissions (e.g., Label 4 to Label 7 in Fig. 3), an SIC decoding order classifier is further employed to intelligently and swiftly determine the SIC decoding order for the detected mixed protocols.

3) SIC Decoding Order Classifier: Denote the number of signal components for one sampling window as N, we propose two neural network structures for implementing the SIC decoding order classifier.

Single Classifier Structure: A single classifier can be designed to predict the SIC decoding order for the scenario of N mixed signals. For instance, when N = 3, the number of all possible SIC decoding orders is 16. It can be shown that this number grows approximately as $O\left(\frac{N}{\ln(N+1)}\right)^N$ [12]. Consequently, this approach results in a massive number of training parameters in one neural network.

Multi-stage Classifiers Structure: To address the complexity of the single classifier structure, we propose a hierarchical model consisting of multi-stage classifiers. Fig. 4 provides an example of the multi-stage SIC decoding order classifier for $N = 3$, where the decoding order is Wi-Fi $\rightarrow$ LTE $\rightarrow$ 5G NR. In this structure, each stage of the classifier predicts which

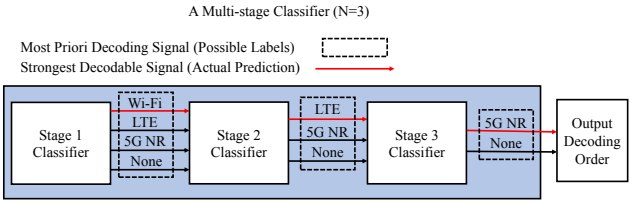

Fig. 4: An example of the multi-stage SIC decoding order classifier with $N = 3$, where the decoding order is Wi-Fi $\rightarrow$ LTE $\rightarrow$ 5G NR.

signal (Wi-Fi, LTE, or 5G NR) can be successfully decoded, given the prior decoding information. If the first stage predicts that decoding is successful for the strongest protocol, then another classifier is used to determine the next signal to be decoded. This process continues until the SIC decoding order for all signals is determined, or none of the signals can be decoded in any stage of the classifier.

4) Decoding Latency Reduction of DL-SIC: As mentioned previously, although T-SIC$_2$ decodes all packets in real-time, it suffers from a high decoding BER due to a fixed decoding order. Therefore, this paper focuses on analyzing the decoding latency of T-SIC$_1$ and DL-SIC, and comparing the decoding BER of T-SIC$_2$ with DL-SIC in Section III.

Best-Case Scenario for T-SIC$_1$: Low decoding latency of T-SIC$_1$ is achieved when the packet detection order matches the successful decoding order. Fig. 5(a) illustrates this scenario, where Packet 1 is the first to arrive and be detected by T-SIC$_1$ among three packets. The dashed "P" block in the figure represents packet detection. If RSS$_1$ > RSS$_2$ > RSS$_3$, Packet 1 can be successfully decoded. Once Packet 1 is decoded and reconstructed, the T-SIC$_1$ receiver can proceed with detecting and decoding the remaining packets. Thus, the decoding latency of Packet 2 under this scenario is:

$$\tau_2(\text{T-SIC}_1) = t_{1,d} + t_{1,c} - a_2, \tag{2}$$

where $t_{1,d}$ and $t_{1,c}$ represent the delay for decoding and reconstructing Packet 1, respectively. a_2 is the difference between the arrival time of Packet 2 and Packet 1.

We next analyze the decoding latency of DL-SIC in this scenario. As shown in Fig. 5(b), DL-SIC detects a weak Packet 2 at t_1 and determines the decoding order, which first decodes Packet 1 and then Packet 2. The resulting decoding latency of Packet 2 can be expressed as:

$$\tau_2(\text{DL-SIC}) = t_{\text{DL}} + \frac{w}{L_1}(t_{1,d} + t_{1,c}) - a_2, \tag{3}$$

where t_{DL} is the processing latency of the DL-SIC, including the testing latency of the protocol detector and the SIC decoding order classifier. w is the sampling window size. L_1 is the packet length of Packet 1. $\frac{w}{L_1}t_{1,d}$ and $\frac{w}{L_1}t_{1,c}$ represent $t'_{1,d}$ and $t'_{1,c}$ in Fig. 5(b), which are the time needed to decode and reconstruct Packet 1, respectively, during each sampling window.

Worst-Case Scenario for T-SIC$_1$: Fig. 6(a) illustrates the worst-case scenario for T-SIC$_1$, where the packet detection

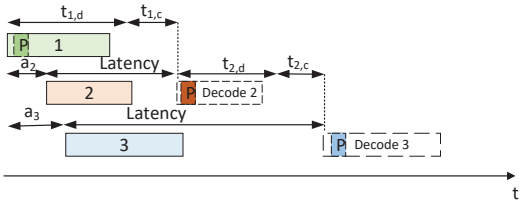

(a) T-SIC$_1$ receiver

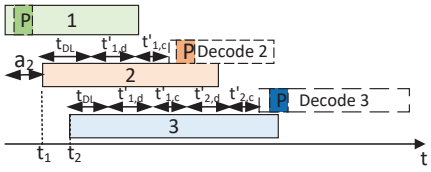

(b) DL-SIC

Fig. 5: Best-case scenario for T-SIC$_1$: RSS$_1$ > RSS$_2$ > RSS$_3$.

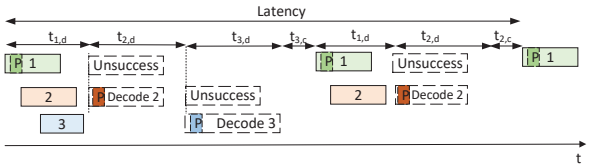

(a) T-SIC$_1$ receiver

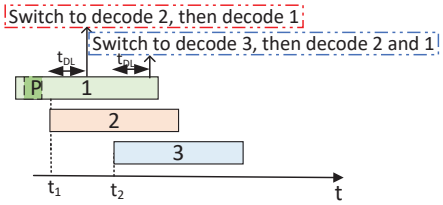

(b) DL-SIC

Fig. 6: Worst-case scenario for T-SIC$_1$: RSS$_1$ < RSS$_2$ < RSS$_3$.

order is reversed compared to the successful decoding order. We analyze the decoding latency from the perspective of Packet 1. Packet 1 is detected first, so the T-SIC$_1$ receiver proceeds to decode Packet 1 and finds that the decoding is unsuccessful due to subsequent strong overlapping transmissions (e.g., Packet 2 and Packet 3 start to transmit during Packet 1), resulting in a decoding latency of $t_{1,d}$. The T-SIC$_1$ receiver then attempts to decode the second detected Packet 2, which is still unsuccessful until it finds that Packet 3 should be decoded first. Therefore, the decoding latency of Packet 1 in this scenario for T-SIC$_1$ can be obtained by summing up the latency of all the above and is given by:

$$\tau_1(\text{T-SIC}_1) = 2t_{1,d} + 2t_{2,d} + t_{2,c} + t_{3,d} + t_{3,c}. \tag{4}$$

The DL-SIC, on the other hand, can quickly detect a stronger signal at time t_1, as illustrated in Fig. 6(b). Consequently, after a latency of t_{DL}, the DL-SIC switches to decode Packet 2. Similarly, it switches to the updated decoding order at time $t_2 + t_{\text{DL}}$ if Packet 3 arrives at t_2. Therefore, the decoding latency of Packet 1 can be expressed as:

$$\tau_1(\text{DL-SIC}) = 2t_{\text{DL}} + \frac{w}{L_3}(t_{3,d} + t_{3,c}) + \frac{w}{L_2}(t_{2,d} + t_{2,c}). \quad (5)$$

III. Simulation Results

To train our neural network models in a supervised manner, we construct labeled datasets by generating Wi-Fi 802.11ac, LTE, and 5G NR waveforms using MATLAB WLAN, LTE, and 5G communication toolboxes. All three waveforms have the same bandwidth of 20 MHz. Each packet is transmitted with one of the four MCS options: (QPSK, $1/2$ rate), (QPSK, $3/4$ rate), (16-QAM, $1/2$ rate), (16-QAM, $3/4$ rate). We generate 3000 samples for each label, and randomly split the dataset into 60%, 20%, and 20% for training, validation, and testing, respectively. We use Keras to build our neural networks, with a maximum training epoch of 50. In addition, early stopping (with patience = 5) is applied to prevent overfitting. We assume that the arrival time of Wi-Fi, LTE, and 5G NR packets follows a Poisson distribution, while the wireless channel of each waveform follows a Rayleigh fading model. We also assume that the three transmitters (Wi-Fi, LTE, and 5G NR) have the same distance to a common DL-SIC receiver. Additionally, the transmission power of each packet for all three protocols is uniformly sampled from a range of [8, 23] dBm [1], [13]. The datasets is available on the website[2].

A. Performance of Protocol Detector

Fig. 7(a) shows the impact of different sampling window sizes (w) on the overall classification accuracy of the protocol detector. As expected, the classification accuracy increases as w increases. All three neural networks achieve over 90% classification accuracy when w is 1024.

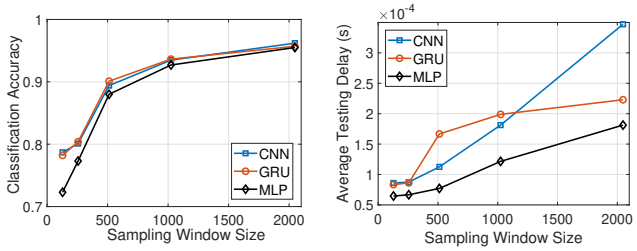

(a) Classification accuracy (b) Average testing delay

Fig. 7: Classification accuracy and average testing delay for various DNN protocol detectors.

In addition to the accuracy, we also consider the impact of the window size on testing delay, which is related to t_{DL} in Eq. (3). The tests for all three neural networks are conducted on an Intel CPU i9-10900K. Fig. 7(b) illustrates the average testing delay for the DNN protocol detector under different w. As w increases, the required testing time for DNN protocol detectors also increases. The GRU model takes more time to test the sample than the other two models when w is less than or equal to 1000. On the other hand, the CNN model takes the longest time when w exceeds 1000. Among all three models, the MLP requires the least testing time under all window sizes.

[2]wireless.ece.arizona.edu/software

B. Performance of SIC Decoding Classifier

Fig. 8 illustrates how the window size (w) affects both the classification accuracy and average testing delay of SIC decoding order classifiers implemented with a CNN architecture. As shown, both classification accuracy and testing delay increase as w grows. This trade-off between accuracy and processing delay suggests the importance of the window size selection for the given application. Additionally, it is worth noting that the total testing delay of multi-stage SIC decoding order classifiers is generally higher than that of single classifier structure.

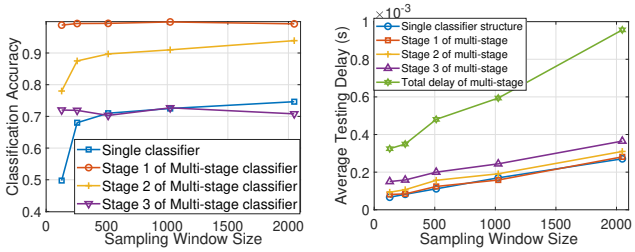

(a) Classification accuracy (b) Average testing delay

Fig. 8: Classification accuracy and average testing delay for SIC decoding order classifiers using CNN architecture.

Fig. 9 illustrates the performance of SIC decoding order classifier with the single classifier structure using different neural networks. We can see that CNN outperforms MLP and GRU in terms of classification accuracy. Moreover, the testing delay for all three neural networks increases as w increases.

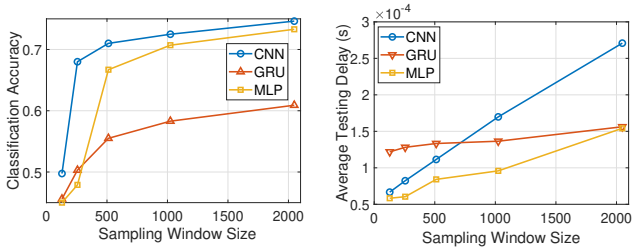

(a) Classification accuracy (b) Average testing delay

Fig. 9: Impact of different neural networks on the SIC decoding order classifier with single classifier structure.

C. Performance Comparison of DL-SIC and T-SIC

Fig. 10(a) shows the impact of w on the average decoding latency of DL-SIC and T-SIC$_1$, based on the analysis presented in Section II-B4. The total process latency of deep learning models (t_{DL}) is obtained by summing the delay of protocol detector and SIC decoding order classifier. The delay for decoding and reconstructing packets (e.g., $t_{1,d}, t_{1,c}$ of Eq.(2)) is obtained using MATLAB. In the best-case scenario, the average decoding latency of T-SIC$_1$ is approximately 0.45 seconds, while DL-SIC achieves a decoding latency of 0.07 seconds when w equals 1024. In the worst-case scenario, T-SIC$_1$ and DL-SIC achieve decoding latency of approximately 0.61 seconds and 0.15 seconds, respectively.

In Fig. 10(b), we compare the decoding bit error rate (BER) of DL-SIC and T-SIC$_2$. We observe that DL-SIC achieves significantly lower BER values for all three protocols, as

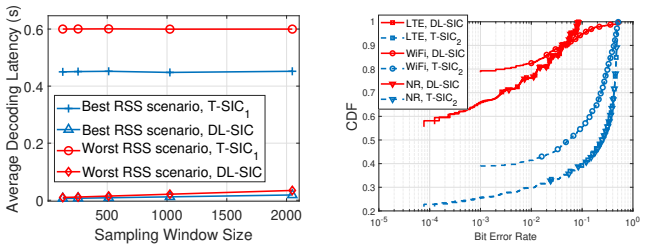

(a) (b)

Fig. 10: (a) Decoding latency of T-SIC$_1$ and DL-SIC; (b) Decoding bit error rate of T-SIC$_2$ and DL-SIC.

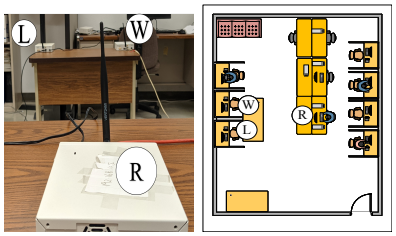

Fig. 11: Experimental setup.

compared to T-SIC$_2$. This is because T-SIC$_2$ cannot obtain the received signal strength (RSS) order information merely by relying on auto-correlations or cross-correlations in T-SIC receivers. It can be observed that with a probability of approximately 60%, DL-SIC reduces decoding BER from 10^{-1} to 10^{-4} compared to T-SIC$_2$.

As mentioned in Section I, there is an inherent trade-off between decoding latency and decoding BER in traditional SIC receivers. Fig. 10 indicates that DL-SIC solves this trade-off and simultaneously achieves low decoding latency and low decoding BER.

IV. Experimental Results

To evaluate the practicality of DL-SIC, we conduct over-the-air (OTA) experiments using a wireless testbed that is comprised of three National Instruments (NI) USRP 2921 devices: an LTE transmitter, a Wi-Fi transmitter, and a DL-SIC receiver (see Fig. 11). We generate Wi-Fi 802.11ac and LTE waveforms using MATLAB toolboxes, as in the simulations. The generated waveforms are then upconverted to a RF channel in the unlicensed band.

We first study the performance of the protocol detector when trained and tested based on the experimental dataset using CNN and $w = 128$. The confusion matrix is shown in Fig. 12. Overall, the protocol detector achieves an average classification accuracy above 78% for all labels.

Next, we evaluate the performance of SIC decoding order classifier. There are five possible labels for the LTE/Wi-Fi coexistence scenario: (1) Signal Undecodable, (2) LTE Decodable Only, (3) LTE $\rightarrow$ Wi-Fi (LTE and Wi-Fi are both decodable with the specified order), (4) Wi-Fi Decodable Only, and (5) Wi-Fi $\rightarrow$ LTE. Fig. 13 shows the confusion matrix of the SIC decoding order classifier with single classifier structure, which accurately predicts all labels with an overall classification accuracy of 88.7%. These results using experimental data demonstrate the practical effectiveness of the proposed DL-SIC classifiers.

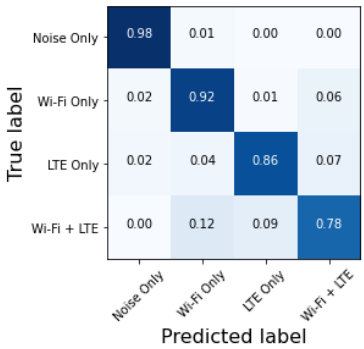

Fig. 12: Confusion matrix of protocol detector, trained and tested with the experimental dataset using CNN and $w = 128$.

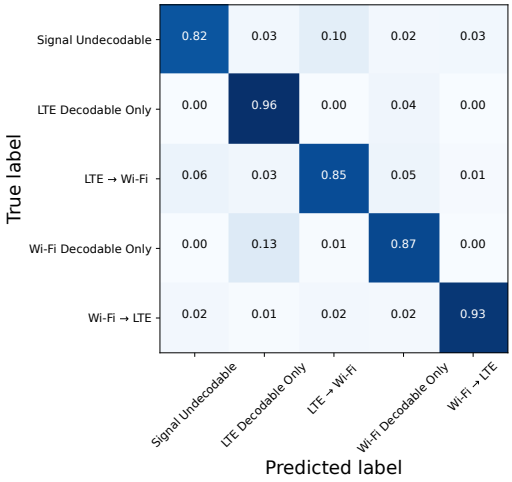

Fig. 13: Confusion matrix of SIC decoding order classifier with single classifier structure, trained and tested with the experimental dataset using CNN and $w = 128$.

V. Related Work

A. Interference Cancellation Techniques

Existing techniques for interference cancellation (IC) belong to two main categories: MIMO and SIC.

Gollakota et al. [14] proposed TIMO, a MIMO-based cross-technology IC technique. It enables an 802.11 receiver to successfully decode Wi-Fi signals even in the presence of interference signals from other technologies by only measuring the interference channel ratio. Yun et al. [4] proposed a MIMO-based receiver that enables decoding of concurrent transmissions of LTE and Wi-Fi signals. Their method employs iterative channel estimation for both LTE and WiFi channels, utilizing the fact there are a small set of LTE channels in the frequency domain that are not interfered by Wi-Fi. Yang et al. [15] introduced ZIMO, enabling harmonious coexistence of ZigBee and Wi-Fi networks.

On SIC, Guo et al. [7] adopted SIC to alleviate the cross-technology interference caused by concurrent transmissions of

LTE and Wi-Fi within unlicensed bands. Yan et al. [6] implemented a single-antenna SIC receiver for Zigbee/Wi-Fi coexistence. Their scheme effectively mitigates the interference from a stronger Wi-Fi signal, thereby facilitating the subsequent decoding of the weaker ZigBee signal. Halperin et al. [8] implemented a SIC receiver to decode simultaneous overlapping transmissions from multiple asynchronous sources. However, these works generally assume prior knowledge of the protocol types for concurrently transmitting packets, or assume the RSS order is known a priori (e.g., the power of Wi-Fi is always stronger than ZigBee).

B. Signal Detection and Classification

Other works focused on detecting the type of interfering technology or modulation scheme [16]–[20]. Hong et al. [16] introduced a framework called DOF, which can accurately detect coexisting radios in the shared spectrum. The authors in [17], [18] proposed deep learning methods for modulation classification. Zha et al. [19] investigated deep learning approaches for both multi-signal detection and modulation classification. The authors in [20] used deep neural networks to detect coexisting signal types based on In-phase/Quadrature (I/Q) samples without decoding them. A common idea underlying these works is that they extract distinctive features from diverse radios for signal detection. However, the above techniques require a significant amount of time to detect signal types, which is not applicable to real-time interference cancellation.

C. Existing Deep Learning-aided SIC Solutions

Some recent works enhanced PHY-layer SIC decoding performance using deep learning techniques. To solve the practical issue that SIC is imperfect in non-orthogonal multiple access (NOMA) systems, authors in [21], [22] proposed a novel approach to approximate SIC decoding functions, such as signal decoding and reconstruction, via deep neural networks. Motivated by the fact that the acquired channel state information (CSI) by the receivers may be inaccurate, the authors in [9], [10] introduced a deep learning-aided SIC, which replaced the interference cancellation blocks of SIC by deep neural networks. However, all the aforementioned works consider homogeneous wireless technologies (where there is only one type of signal), and they assume the SIC decoding order is given or known, which are not applicable to heterogeneous network coexistence.

VI. Conclusions and Future Work

SIC has shown great potential in improving spectrum utilization of cross-technology coexistence, utilizing the power differences of concurrently transmitted signals. In this work, we proposed DL-SIC, a deep learning-aided SIC approach. The simulation results demonstrate that DL-SIC achieves low decoding latency and low decoding BER simultaneously. Extensive simulations and OTA experiments validate the effectiveness and practical feasibility of DL-SIC.

As future work, we will consider multiple links for each protocol to generalize the proposed DL-SIC architecture.

References

[1] 3GPP, "Feasibility study on licensed-assisted access to unlicensed spectrum," Standard (TR) 36.889, 2015.

[2] 3GPP, "3GPP TS 37.213: Physical layer procedures for shared spectrum channel access (release 16)," July 2020.

[3] Y. Gao, X. Chu, and J. Zhang, "Performance analysis of LAA and WiFi coexistence in unlicensed spectrum based on Markov chain," in *Proc. of IEEE Global Communications Conference (GLOBECOM)*. IEEE, 2016, pp. 1–6.

[4] S. Yun and L. Qiu, "Supporting WiFi and LTE coexistence," in *Proc. of the Computer Communications (INFOCOM) Conf.* IEEE, 2015, pp. 810–818.

[5] Z. Guo, M. Li, and Y. Xiao, "Enhancing LAA/Wi-Fi coexistence via concurrent transmissions and interference cancellation," in *Proc. of International Symposium on Dynamic Spectrum Access Networks (DySPAN)*. IEEE, 2019, pp. 1–10.

[6] Y. Yan, P. Yang, X.-Y. Li, Y. Zhang, J. Lu, L. You, J. Wang, J. Han, and Y. Xiong, "WizBee: Wise ZigBee coexistence via interference cancellation with single antenna," *IEEE Transactions on Mobile Computing*, vol. 14, no. 12, pp. 2590–2603, 2014.

[7] Z. Guo, M. Li, and M. Krunz, "Exploiting successive interference cancellation for spectrum sharing over unlicensed bands," *IEEE Transactions on Mobile Computing*, 2023.

[8] D. Halperin, T. Anderson, and D. Wetherall, "Taking the sting out of carrier sense: interference cancellation for wireless LANs," in *Proc. 14th ACM Int. Conf. on Mobile Computing and Networking*, 2008, pp. 339–350.

[9] N. Shlezinger, R. Fu, and Y. C. Eldar, "DeepSIC: Deep soft interference cancellation for multiuser MIMO detection," *IEEE Transactions on Wireless Communications*, vol. 20, no. 2, pp. 1349–1362, 2020.

[10] T. Van Luong, N. Shlezinger, C. Xu, T. M. Hoang, Y. C. Eldar, and L. Hanzo, "Deep learning based successive interference cancellation for the non-orthogonal downlink," *IEEE Transactions on Vehicular technology*, vol. 71, no. 11, pp. 11 876–11 888, 2022.

[11] A. Shewalkar, "Performance evaluation of deep neural networks applied to speech recognition: RNN, LSTM and GRU," *Journal of Artificial Intelligence and Soft Computing Research*, vol. 9, no. 4, pp. 235–245, 2019.

[12] D. Berend and T. Tassa, "Improved bounds on bell numbers and on moments of sums of random variables," *Probability and Mathematical Statistics*, vol. 30, no. 2, pp. 185–205, 2010.

[13] 3GPP, "Standard (TR) 36.889: NR-based access to unlicensed spectrum," 2019.

[14] S. Gollakota, F. Adib, D. Katabi, and S. Seshan, "Clearing the RF smog: making 802.11 robust to cross-technology interference," in *Proc. of the ACM SIGCOMM Conf.*, 2011, pp. 170–181.

[15] Y. Yubo, Y. Panlong, L. Xiangyang, T. Yue, Z. Lan, and Y. Lizhao, "ZIMO: Building cross-technology MIMO to harmonize ZigBee smog with WiFi flash without intervention," in *Proc. 19th Annual Int. Conf. on Mobile computing & networking*, 2013, pp. 465–476.

[16] S. S. Hong and S. R. Katti, "DOF: a local wireless information plane," in *Proc. of the ACM SIGCOMM Conf.*, 2011, pp. 230–241.

[17] T. J. O'Shea, J. Corgan, and T. C. Clancy, "Convolutional radio modulation recognition networks," in *Proc. of International conference on engineering applications of neural networks*. Springer, 2016, pp. 213–226.

[18] T. J. O'Shea, T. Roy, and T. C. Clancy, "Over-the-air deep learning based radio signal classification," *IEEE Journal of Selected Topics in Signal Processing*, vol. 12, no. 1, pp. 168–179, 2018.

[19] X. Zha, H. Peng, X. Qin, G. Li, and S. Yang, "A deep learning framework for signal detection and modulation classification," *Sensors*, vol. 19, no. 18, p. 4042, 2019.

[20] W. Zhang, M. Feng, M. Krunz, and A. H. Y. Abyaneh, "Signal detection and classification in shared spectrum: A deep learning approach," in *Proc. of IEEE Conf. on Computer Communications (INFOCOM)*, 2021, pp. 1–10.

[21] J.-M. Kang, I.-M. Kim, and C.-J. Chun, "Deep learning-based MIMO-NOMA with imperfect SIC decoding," *IEEE Systems Journal*, vol. 14, no. 3, pp. 3414–3417, 2019.

[22] M. A. Aref and S. K. Jayaweera, "Deep learning-aided successive interference cancellation for MIMO-NOMA," in *Proc. of IEEE Global Communications Conference*. IEEE, 2020, pp. 1–5.